Measuring S-phase duration of adult stem cells in the flatworm *Macrostomum lignano* by double replication labelling and quantitative colocalization analysis

Freija Verdoodt[1], Maxime Willems[1], Ineke Dhondt[1], Wouter Houthoofd[1], Wim Bert[1] and Winnok H. De Vos[2,3]

[1] Department of Biology, Ghent University, Ghent, Belgium
[2] Department for Molecular Biotechnology, Ghent University, Ghent, Belgium
[3] NB-photonics, Ghent University, Ghent, Belgium

Short title:
S-phase & label colocalization in *M. lignano*

Corresponding author:
Verdoodt Freija, Nematology unit, Department of Biology, K.L. Ledeganckstraat 35, 9000 Gent, Belgium
Phone: +32 (0)9 264 87 40
Fax: +32 (0)9 264 53 44
Freija.Verdoodt@ugent.be

Keywords:
cell cycle; colocalization; neoblast; platyhelminthes; regeneration; S-phase

Abbreviations:

Anti-phos-H3	anti-phosphorylated histone H3
CldU	chlorodeoxyuridine
IdU	iododeoxyuridine
T_c	cell cycle duration
T_s	S-phase duration

1. Abstract

Platyhelminthes are highly attractive models for addressing fundamental aspects of stem cell biology *in vivo*. These organisms possess a unique stem cell system comprised of neoblasts, which are the only proliferating cells during adulthood. In this study, the S-phase duration (T_s) of neoblasts was determined, both during homeostasis and regeneration in the flatworm *Macrostomum lignano*. A double immunohistochemical technique was used, performing sequential pulses with the thymidine analogs chlorodeoxyuridine (CldU) and iododeoxyuridine (IdU), separated by variable chase times in colchicine. in the presence of colchicine cell nuclei
Due to the localized nature of the fluorescent signals ~~(nuclei)~~ and variable levels of autofluorescence, standard intensity-based colocalization analyses could not be applied to accurately determine the colocalization. Therefore, an object-based colocalization approach was devised to score the relative number of double-positive cells. Using this approach we found that the S-phase duration in the main population of neoblasts was approximately 13 hours. During early regeneration, no significant change in T_s was observed.

2. Introduction

Proliferation is a fundamental trait of stem cells, as they have the ability to continuously self-renew and generate large numbers of differentiated progeny. This dual function asserts their crucial role during development, tissue homeostasis, and regeneration, and therefore requires meticulous control (Morrison *et al.*, 1997;Morrison and Spradling, 2008). Both external and internal stimuli affect the dynamics of stem cells, a fact that emphasizes the importance of studying these cells in their natural environment (Rando, 2006;Orford and Scadden, 2008). However, *in vivo* stem cell research is often challenging because of experimental difficulties caused by tissue depth and motion artefacts (Tsai *et al.*, 2002;Tanaka, 2003). Mainly for this reason, Platyhelminthes have been amply introduced as highly attractive model organisms for addressing fundamental aspects of stem cell biology *in vivo* (Newmark and Sánchez Alvarado, 2002;Sánchez Alvarado, 2004). These organisms possess a unique stem cell system within the animal kingdom, comprised of neoblasts that are the only proliferating cells in adult species (Baguñà, 1981;Saló and Baguñà, 2002;Sánchez Alvarado, 2007;Ladurner *et al.*, 2008;Agata and Umesono, 2008). Although neoblasts are a powerful model for studying proliferation dynamics of a population of adult stem cells *in vivo*, fundamental information on specific parameters of the cell cycle is relatively limited. To our knowledge, other than the mean duration of the G2-phase in *Schmidtea mediterranea* and *Macrostomum lignano* (Newmark and Sánchez Alvarado, 2000;Nimeth *et al.*, 2004;Nimeth *et al.*, 2007), and the total cell cycle duration (T_c) in *S. mediterranea* (Kang and Sánchez Alvarado, 2009), no specific parameters of other phase durations are available. Furthermore, regeneration has been shown to temporarily affect the numbers of S-phase and mitotic cells in flatworms, indicating adjustment of the cell cycle kinetics (Saló and Baguñà, 1984;Newmark and Sánchez Alvarado, 2000;Nimeth *et al.*, 2007;Wenemoser and Reddien, 2010;Verdoodt *et al.*, 2012a). However, it is not completely understood at what stage the cell cycle is adapted during this process.

In the past, the combined use of two different thymidine analogs has been demonstrated as a valuable technique for determining kinetic parameters of cycling cells (Wimber and Quastler, 1963;David and Campbell, 1972;Miller *et al.*, 1991;Yanik *et al.*, 1992;Rachel *et al.*, 2002;Hayes and Nowakowski, 2002;Burns and Kuan, 2005). Performing sequential pulses with such analogs allows for determining the duration of the S-phase (T_s) of the cell cycle. A method for immunohistochemical detection of two thymidine analogs, chlorodeoxyuridine (CldU) and iododeoxyuridine (IdU), has been established for the flatworm *Macrostomum lignano* (Verdoodt *et al.*, 2012b). In the study presented here, this method was adapted to test the T_s of neoblasts during homeostasis and regeneration in *M. lignano*. To this end, individual worms received sequential pulses with CldU and IdU, which were separated by varying chase times in colchicine. The use of colchicine, which inhibits cell cycle progression at metaphase (Nagl, 1972), allowed analysis of a single round of cell proliferation and avoided misinterpretation due to cell doublings. To determine T_s, overlap between the two markers was evaluated. Due to the localized nature of the fluorescent signals in limited regions (nuclei) of the image, standard intensity-

based colocalization analyses which evaluate the whole image, could not be applied. Instead, an object-based colocalization approach was devised to score the relative number of double-positive cells. Using this approach, the duration of S-phase in the main population of neoblasts was determined to be approximately 13 hours, both during homeostasis and early regeneration.

3. Materials and methods

3.1. Animal culture and amputation of the rostrum

Cultures of *M. lignano* were reared in f/2-medium (Egger and Ishida, 2005) and fed *ad libitum* with the diatom *Nitzschia curvilineata,* as described previously (Schärer *et al.*, 2007;Ladurner *et al.*, 2008). To induce regeneration, the rostrum was amputated at the level anterior to the brain. Amputations were performed with a fine steel surgical blade (SM62; Swann-Morton) under a stereo microscope, while worms were relaxed in a small droplet of 1:1 $MgCl_2.6H_2O$ (7.14%) and ASW (artificial sea water). Immediately thereafter, specimens were washed in f/2-medium and pulsed with CldU.

3.2. Accumulation of mitotic cells after colchicine incubation

To test the efficiency and toxicity of colchicine in *M. lignano*, the accumulation of mitotic cells was analysed after incubation with different concentrations of colchicine, using anti-phosphorylated histone H3 (anti-phos-H3). Adults were incubated in a colchicine-containing medium (Sigma-Aldrich) of 0.001%, 0.005%, or 0.010% (in f/2-medium). After 3h, 24h, 48h and 6d of incubation, mitotic cells were visualized using rabbit-anti-phosphorylated histone H3 (Upstate Biotechnology) and TRITC-conjugated swine-anti-rabbit (DAKO), according to the method described earlier (Verdoodt *et al.*, 2012a). For each condition, 4 replicates were analyzed.

3.3. CldU- and IdU-pulse and immunocytochemistry

For the first pulse, uncut animals or regenerates were incubated in CldU (10 mM in f/2-medium, 30 min, in the dark; Sigma-Aldrich). From this moment on, animals were protected from light. Specimens were then rinsed with f/2-medium, and chased in colchicine-containing medium (0.005% in f/2; Sigma-Aldrich) for 0 h, 1 h, 2 h, 4 h, 6 h, 12 h, 24 h, and 48 h. Subsequently, the second pulse was performed with IdU (1mM in colchicine-containing medium, 30 min; Sigma-Aldrich), followed by washing with colchicine-medium (2 x 5 min). Relaxation, fixation, and indirect visualization of both CldU and IdU were performed as described previously (Verdoodt *et al.*, 2012b). The set of antibodies used for indirect visualization of CldU were rat-anti-CldU (AbD Serotec) and FITC-conjugated donkey-anti-rat (Rockland). For indirect visualization of IdU, mouse-anti-IdU (Becton-Dickinson) and Alexa Fluor 568-conjugated goat-anti-mouse (Invitrogen) were used.

3.4. Image Acquisition

For the visualization of CldU- and IdU-label, a Nikon C1 (Nikon Instruments, Paris, France) confocal laser scanning microscopy system was used mounted on a Nikon TE2000 (Nikon Instruments, Paris, France) inverted epifluorescence microscope, equipped with a 488-nm Multi-line Ar laser and 543nm HeNe laser. CldU and IdU signals were sequentially excited with both laser lines (by line-scanning) and detected through a 515/30 nm bandpass filter, and a 570 long pass combined with a 593/40 nm bandpass filter, respectively. All images were acquired using identical settings of laser power, detector gain and offset. 3D-images were acquired with the pinhole set at 1AU, using a Plan Fluor 60x/1.4 oil lens at a voxel size of 0.41x0.41x1.0 µm3.

3.5. Image Analysis

All images were acquired with Nikon EZ-C1 software (Nikon Instruments, Paris, France). Visualization, annotation and quantification of images were performed with Fiji, a packaged version of the open source program ImageJ (W. Rasband, National Institutes of Health, Bethesda, Maryland, USA). For determination of double-positive nuclei in each specimen, an object-based colocalization analysis was developed. Assuming that a positive replication labelling yields a signal that fills up the

entire nucleus, circularity and size were used as limiting parameters. The following steps were performed. First, a selection was made for analysis of the relevant 3D region of interest. In each animal, the region anterior to the testes and the region posterior to the female genital pore were analyzed. For each condition, between 4 and 7 replicates were analyzed. A sum projection was made of the Z-slices, and the individual channels were pre-processed by sequential background subtraction (radius = 20µm), Gaussian filtering (sigma = 1µm) and median filtering (radius = 2µm). Next, objects (nuclei) were specifically enhanced in both channels by applying a Laplace filter with automatic scale selection (as documented before by De Vos *et al.*, 2010) and segmented by global isodata autothresholding. To compensate for closely-located nuclei, the resulting masks were used to extract objects, which were further separated by maxima finding and region growing. By particle analysis, those objects that did not comply with user defined nuclear shape criteria (size and circularity) were removed. Finally, colocalization was determined by scoring, per object, the amount of overlap between the binarized and coded versions of the two channels. Objects in the first channel were coded with the number 1, objects in the second channel were coded with the number 2, and so overlapping regions have code 3. Signals were said to colocalize for a given ROI, when the number of overlapping pixels (code 3) was larger than 50% of the total number of pixels of the object of interest. Finally, the raw output was visually verified and, if necessary (e.g. in spatially restricted zones of high autofluorescence), corrected using a dedicated ROI correction/deletion tool. The workflow of the object-based colocalization analysis is summarized in Figure 1. The code is freely available at the following URL: http://www.limid.ugent.be/software.htm. At least 4 ~~individual~~s were analysed per condition (n=4-7). For validation, the object-based analysis was compared to intensity-based colocalization methods using Pearson or Manders coefficients (Bolte and Cordelieres, 2006;Manders *et al.*, 1992).

individual organisms

3.6. Statistical Analysis

The statistical analysis was done using Statistica 7 (StatSoft Europe GmbH, Hamburg, Germany). Normality and homogeneity of variances were tested using a Kolmogorov-Smirnov test and a Levene's test, respectively. $CldU^+$ data (absolute numbers) were square root transformed, prior to analysis. Proportions of $CldU^+$ /IdU^+ cells were first square root and then arcsinus transformed (Sokal and Rohlf, 1995). The obtained data were analyzed by means of one-way analysis of variance (ANOVA), followed by a post-hoc Bonferroni test. Linear regression analysis was performed on the individual samples assayed at 0 h, 1 h, 2 h, 4 h, and 6 h, using the proportion of double labelled cells and the chase time duration as independent and dependent variable, respectively.
Data that did not meet the assumption for homogeneity of variances were analyzed using a non-parametric Mann-Whitney U test (pair wise comparison between homeostasis and regeneration).

4. Results

4.1. Validation of the colocalization analysis

First, the colocalization analysis was validated on a number of control images, including single-pulsed samples as well as simultaneously double-pulsed samples. A comparison was made with the typical colocalization metrics Pearson correlation coefficient and Manders coefficients. While on average, the Pearson correlation coefficient was close to 0 in single stained samples and relatively high for double stained samples (0.8), the values for the Manders coefficients were not straightforward (Table 4.1). This is plausibly due to the presence of autofluorescent components, which cannot be removed in classical intensity-based analyses. Moreover, neither the Pearson nor the Manders coefficients returned the exact information that was required, namely the number of double positive nuclei, relative to the total number of labelled nuclei. The object-based method effectively segments only those objects that comply with the nuclear shape requirements and accordingly provided the necessary output. Using this method, average colocalization values of 0% in single-pulsed samples and 92% in double-pulsed samples were obtained. Comparison of the raw output with values after manual correction (Table 4.1) shows that the differences are negligible and indicates that the false-negative rate in double stained samples was not due to analytical errors but rather to labelling inefficiencies.

4.2. S-phase duration during homeostasis

The T_s of neoblasts was determined by performing sequential pulses with the thymidine analogs CldU and IdU, separated by varying chase times in colchicine-containing medium. Prior to performing these experiments, three concentrations of colchicine (0.001%, 0.005%, and 0.010%) were tested for their efficiency and toxicity in *M. lignano,* by analyzing the accumulation of mitotic cells. For each concentration, the number of anti-phos-H3 labeled cells was quantified, after an incubation period of 3h, 24h, 48h, and 6d (supplementary Figure S1). The median concentration (0.005%) demonstrated a faster and more efficient blocking after short incubations, while no toxic effect was obvious for incubations up to 48h. The highest concentration on the other hand, demonstrated observed a toxic effect after 24 h of incubation. In conclusion, the use of a 0.005% solution of colchicine demonstrated the best balance between efficiency of blocking cells in M-phase on one hand, and no dramatic toxic effect for exposures up to 48 h. Hence, this concentration was used for further experiments.

To estimate the T_s of neoblasts, adults were pulsed for 30 minutes with CldU, chased in CldU-free, colchicine-containing medium, and subsequently pulsed for 30 minutes with IdU. Individuals were then fixed and both analogs were visualized by double immunofluorescence labelling. First, absolute numbers of $CldU^+/IdU^+$, $CldU^+/IdU^-$, and $CldU^-/IdU^+$ nuclei were quantified (see supplementary Figure S2a), using the aforementioned object-based colocalization analysis. The number of $CldU^+$ cells remained at a constant level up to 6 h chase (one-way ANOVA, $p>0.05$). After 12 h chase, a marginally significant increase (one-way ANOVA, $p=0.046$) was observed in the total amount of $CldU^+$ cells (single and double labelled). After 24 h chase, a highly significant increase (one-way ANOVA , $p<0.01$) was measured in the number of $CldU^+$ cells. This increase can be explained by a small proportion of cells that may have been ~~were~~ still unaffected by the colchicine and were able to divide.
Second, the proportion of $CldU^+/IdU^+$ neoblasts was determined by the ratio of $CldU^+/IdU^+$ nuclei over the total amount of $CldU^+$ nuclei (both single- and double-labelled). In this paradigm, nuclei from cells that have exited S-phase, during or after the first pulse, will be $CldU^+/IdU^-$ (Figure 2a). The chase time after which all CldU-labelled cells $CldU^+/IdU^-$ corresponds to the maximal T_s. The mean proportion of $CldU^+/IdU^+$ neoblast nuclei was quantified in individual organisms (the region anterior and posterior of the gonads) after chase times of 0 h, 1 h, 2 h, 4 h, 6 h, 12 h, 24 h, and 48 h (Figure 2b-c). An initial fast decrease in the proportion of double-labelled nuclei was observed. After 0 h chase, 94% (±3, n=5) $CldU^+/IdU^+$ nuclei were quantified. After 1 h chase, 88.26% (±2.1, n=4) double labeled nuclei were present, and after 2 h chase, this number had decreased significantly to 69% (±6, n=5; one-way ANOVA, $p=0.002$). The fast rate ~~by~~ with which the proportion of $CldU^+/IdU^+$ cells diminished, ~~was~~ continued for chase times up to 12 h: 4 h, 6 h, and 12 h resulted in proportions of 64% (±3, n=5), 50% (±3, n=7), and 21% (±7, n=4), respectively. For chase times longer than 12 hours, the number of double-positive nuclei further decreased, albeit at a slower rate. A chase of 24 h and 48 h resulted in a proportion of 14% (±4, n=5) and 3% (±1, n=5) $CldU^+/IdU^+$ cells, respectively. The presence of this second phase in the graph is most likely linked to the increase in total number of $CldU^+$ cells (see discussion). Therefore, for estimation of T_s, only results up to 6 h chase were taken into account. These time points (0 h, 1 h, 2 h, 4 h, and 6 h) were used in a regression analysis. The intersection of this trendline ($R^2=0.93$) with the X-axis was used as a measure for the duration of S-phase (Figure 2d). Here a duration of 12.7 hours was measured.

4.3. S-phase duration during regeneration

Previously, amputation of the rostrum in *M. lignano* has been shown to cause an immediate increase in the number of S-phase cells after amputation. Thirty minutes after amputation, this number had already risen by 28%, demonstrating that a significant amount of cells were induced to enter S-phase due to amputation (Verdoodt *et al.*, 2012a). Therefore, in this study, cells that were in S-phase during the 30-minute time interval after amputation, were followed as they progressed through the DNA synthesis phase. To this end, individuals were amputated at a region ~~the level~~ anterior to the brain (Figure 3a, upper panel), after which the same experimental set-up was used as for the homeostasis experiment

(Figure 3a, lower panel). Subsequently, CldU and IdU were visualized (Figure 3c) and the proportion of $CldU^+/IdU^+$ neoblasts was determined (Figure 3b, for absolute numbers see supplementary Figure S2b). Similar to the results observed during homeostasis, the proportion of double-labeled nuclei decreased rapidly for chases up to 12 hours. After 0 h, 2 h, 4 h, and 12 h chase, a proportion of 84% (±0.03, n=4), 73% (±0.08, n=4), 57% (±0.03, n=5), and 24% (±0.03, n=4) was quantified, respectively. Longer chase times demonstrated a slower decrease of the proportion of $CldU^+/IdU^+$ cells: 24 h and 48 h chase resulted in 8% (±2, n=5) and 11% (±3, n=4) double-labelled cells, respectively.
Results obtained from regenerating individuals were compared with corresponding chase time durations from the homeostasis experiment. No significant differences were found (Mann-Whitney U, $p>0.05$), except for 48 h chase ($p=0.03$). These results indicated that amputation of the rostrum did not result in an acceleration of the S-phase during early regeneration.

5. Discussion

In this study, the S-phase of cycling neoblasts was studied in *M. lignano* by means of a double labelling technique using two different thymidine analogs (CldU and IdU) and the mitotic blocking agent colchicine. Colchicine was used to prevent labelled cells from dividing and entering the S-phase of a subsequent cycle. The necessity of blocking the cell cycle of labelled cells is indicated by previous studies, demonstrating that (1) neoblasts cycle asynchronously, and that (2) subpopulations of neoblasts exist with different cell cycle kinetics (Ladurner *et al.*, 2008). Given that cycling of neoblasts is not synchronized, cells that incorporate CldU during the first pulse are at different stages of the S-phase. Since T_c is unknown in *M. lignano*, $CldU^+$ cells going through mitosis while others are still in S-phase is a possibility that should be taken into account. Furthermore, diverse cell kinetics in subpopulations of neoblasts have been shown by Nimeth et al. (2007). In this study the presence of a small proportion of fast-cycling neoblasts was observed, which can traverse from the beginning of S-phase, through G2-phase, and into M-phase in merely two hours. On the other hand, the main population of neoblasts was observed to cycle much slower and needed four hours to merely traverse the G2-phase. These diverse kinetics suggest that fast-cycling $CldU^+$ cells could already go through mitosis and even enter a new S-phase, while slower cycling $CldU^+$ cells have not yet left the initial S-phase. Both processes affect the slope of $CldU^+/IdU^+$ cells in that cell division affects the total number of $CldU^+$ cells, and entrance into a new round of DNA-replication results in IdU-uptake. Therefore, in order to analyse the duration of the S-phase, it is necessary to block cells in metaphase. By comparing different concentrations, the 0.005% colchicine solution demonstrated a good balance between efficiency of blocking cells in metaphase on one hand, and experiencing no dramatic toxic effects for exposures up to 48h (Supplementary Figure S1). This concentration is acceptable, as it should not interfere with regular cell cycle progression. Indeed, at concentrations ranging from 0.0002% to 0.2%, colchicine has been reported to have no measurable effect on the rate of DNA synthesis, nor on the rate of progression to M-phase in plant cells, and human cells in culture (Taylor, 1965;Borisy and Taylor, 1967;Villemont *et al.*, 1997). Furthermore, in *M. lignano* colchicine (0.005%) has been shown to have no effect on the progression of cycling neoblasts through S-phase. This was demonstrated by similar rates of cells cycling from S-phase to M-phase in both colchicine-treated animals and non-treated animals (Nimeth *et al.*, 2004).
To determine T_s, the number of double-labelled cells was scored in a pulse chase experiment with increasing chase times. Due to the localized nature of the fluorescent signals (nuclei) and variable levels of autofluorescence, standard intensity-based colocalization analyses could not be applied to accurately determine the colocalization. Moreover, most classical analyses fail to return the desired quantitative information, i.e. a number of double-positive nuclei. Hence, an object-based colocalization approach was devised to score the relative number of double-positive cells within a sample. This method, which is based on scoring the overlap between the segmented and binarized nuclear ROIs of both channels, proved robust and reliable, as demonstrated in both single- and double-labelled control images. With minor modifications, this method should be applicable to various biological image data-sets. Through the modification of the parameters, such as the degree of overlap, the analysis should also be able to deal with differences in labelling efficiency.

Maybe you should mention that there is a small risk of incomplete blocking as shown

Theoretically, in this paradigm, the chase time for which all CldU-labelled cells have left S-phase, and are therefore $CldU^+/IdU^-$, corresponds to the maximum T_s (Figure 2a). In this study, the number of double labelled cells decreased quickly. Surprisingly, though, the initial steep decrease of the curve, was followed by a second phase with a considerably slower decrease (Figure 2c). The presence of this phase may be due to a subpopulation of slow-cycling cells with an extended S-phase duration (>48h) compared to the main cycling population, or due to technical factors. To evaluate the latter possibility, the efficiency of colchicine, which is reflected by absolute numbers of $CldU^+$ cells, was tested (Suppelementary Figure S2). These numbers of CldU-labelled cells (both single and double labelled) were observed constant for chase times up to 6 h. Increasing the chase time by another six hours, however, resulted in a small increase ($p=0.046$), which was observed to be even larger at 24 h chase ($p<0.01$). The expanded number of $CldU^+$ cells after long chase times, can be explained by a small amount of labelled cells that were able to divide, separating their label over two daughter cells. Double labelling of such cells, due to entry into the S-phase of a new cell cycle, explains the delayed decrease of $CldU^+/IdU^+$ cells for longer chase times. Another possible explanation for the increased number of $CldU^+$ cells is a toxic effect of colchicine after prolonged cell cycle arrest, and re-uptake of the analog by other cells. So far, it is not clear which of both hypotheses is correct. However, due to this technical constraint, results for chase times of 12 h and longer, were not used for analysis of S-phase duration. For chase times up to 6 h, though, efficient blocking of cells in metaphase is demonstrated by the constant number of $CldU^+$ cells. Hence, regression analysis was performed on results obtained from animals that were chased for 0 h, 1 h, 2 h, 4 h, and 6 h (Figure 2d). Based on these data points, T_s was estimated to be approximately 13 hours. Although S-phase duration varies greatly among different taxa, the phase length observed, here lies within range of the S-phase duration in, for instance, hydra (12-15 h) and rat satellite cells (14 h) (David and Campbell, 1972;Schultz and McCormick, 1994).

In *M. lignano,* the presence of a population of fast-cycling neoblasts has been described, additional to the main population of cycling neoblasts (Nimeth *et al.*, 2007). These fast-cycling cells were observed to cycle through the whole S-, and G2-phase in merely 2 hours. The presence of a subpopulation of neoblasts with a considerably shorter S-phase compared to the main population, is expected to result in an even steeper decline in the first phase of the graph. Based on our data, however, no clear indication for such a subpopulation can be deduced. However, it should be noted that this can be caused by (1) their low incidence within the neoblast population, and (2) their extremely short Ts (1-2 h) which hampers their discrimination. Furthermore, an S-phase duration of less than 2 h has also been observed during embryonic development in *M. lignano* (Willems *et al.*, 2009). Although separate phase durations were not determined, cell lineaging experiments have demonstrated cleavage of blastomeres approximately every one to two hours. Similar to *M. lignano*, in other models a considerable elongation of the S-phase in adults, compared to embryos, has been observed (Alexiades and Cepko, 1996). Altogether, it can be concluded that, although a fast passage through S-phase (< 2 h) is possible in *M. lignano*, the majority of cycling neoblasts in adults need approximately 13 h.

To evaluate S-phase duration during regeneration, individuals were amputated at the level of the rostrum. Previously, during regeneration of this region, an immediate expansion of S-phase numbers was demonstrated, indicating an early-onset increase in cell proliferation (Verdoodt *et al.*, 2012a). In this study was tested whether an acceleration at the level of the S-phase is responsible for these adjusted cell cycle kinetics. To this end, the T_s of cells that are in S-phase after amputation, was evaluated and compared to the situation during homeostasis. The data, obtained by our double labelling experiment, demonstrate that amputation did not considerably affect the S-phase duration. The curve of the proportion of double-labelled cells in regenerating animals demonstrated kinetics, comparable to those observed in non-regenerating animals (Figure 3b). Again, an initial steep decrease was observed, which showed no significant differences with time-point matched counterparts in homeostasis. Based on this observation, it can be concluded that S-phase was not accelerated during early regeneration. Hence, other adjustments of the cellular kinetics within the neoblast pool must occur to account for the early-onset proliferation boost after amputation. Cell production depends on the number of dividing cells and their average cell cycle duration (West *et al.*, 2004). Thus, the fast replacement of missing tissue during regeneration in *M. lignano*, can be supported by an expansion of the pool of cycling neoblasts, an acceleration of a cell-cycle phase other than the S-phase, or both. In the same way, in mouse epidermis cells, the wave of cells entering S-phase upon induction of regeneration, is caused by a significantly shortened G1-phase, rather than a reduction of the S-phase

duration. Additional studies should be done to further address cell cycle kinetics during regeneration in *M. lignano*.

In this study, for the first time, the S-phase duration was determined in a flatworm model, during both homeostasis and regeneration. These results add up to the limited knowledge on the cell cycle dynamics of flatworms, and will contribute to a better understanding of cell cycle regulation in these organisms. Furthermore, a standardized object-based method was established for colocalization analysis. This method will be of further use when applying double immunohistochemical labelling techniques, and thus serve as a valuable expansion of the toolbox for studying flatworm stem cells *in vivo*.

6. Acknowledgements

The authors want to thank Peter Ladurner and Bernhard Egger for establishing the double labelling protocol in *M. lignano*. Furthermore, we want to thank Marjolein Couvreur for help with the cultures of *M. lignano*.

7. Funding

FV and MW received funding from the Institute for the Promotion of Innovation through Science and Technology in Flanders (IWT-Vlaanderen).

8. Figure legends

Figure 1: Object-based colocalization for scoring of double-labelled nuclei in tissue sections of *M. ligano*.
(a) Workflow demonstrating the major aspects of the analysis; (b) Criterion for determing overlap in a ROI; (c) Example composite image of CldU (red) and IdU (green) labelled nuclei in a gut section of *M. lignano*; (d) The same image after segmentation and binarization; (e) The same image with segmented nuclei outlined, double-positive nuclei with a yellow contour. Scale bars: 10 µm.

Figure 2: Determination of T_s during homeostasis.
(a) Scheme of the experimental set-up. Animals were pulsed with CldU (30 min), chased for various durations in colchicine and subsequently pulsed with IdU (30 min). Demonstrated are four hypothetical cells (I, II, III, and IV) at a different stage of S-phase during the first pulse (top panel). With longer chase times, there is an increased chance that cells have already left S-phase and therefore do not incorporate the IdU-label. (b) Visualization of CldU (green) and IdU (red) labeling in whole mount animals (confocal images) after 0h, 4h, and 24h chase. After 0h chase, the majority of cells are double labeled (yellow). Note the gradually decreasing amount of double labeled cells after 4h and 24h chase. Anterior is to the left. Scale bars: 50µm. (c) Graph representing the mean proportion (±SEM, n=4-7) of $CldU^+/IdU^+$ cells within the whole population of $CldU^+$ cells (single- and double-labelled). Note the steep decrease for chase times up to 12 hours. (d) Linear regression analysis based on data for 0 h, 1 h, 2 h, 4 h, 6 h, and 12 h chase (n=4-7). The regression line (black line) intersects with the X-as at 12.7 h, which is an estimation of T_s.

Figure 3: T_s, compared between homeostasis and early regeneration.
(a) Scheme of adult *M. lignano* (upper panel) depicting the amputation level (dotted red line). The rostrum is depicted by the 2-sided arrow. b, brain; e, eye; t, testis; o, ovary. Scheme of the

experimental set-up (lower panel). amp, amputation; fix, fixation. (b) Graph representing the mean proportion (±SEM, n=4-7) of $CldU^+/IdU^+$ cells after various chase times during homeostasis (blue curve) and regeneration (black curve). Note the similar course of both curves, only after 48 h of chase a significant difference (asterisk) was observed. (c.) Visualization of CldU (green) and IdU (red) labeling in whole mount animals (confocal images) after 0 h, 4 h, and 24 h chase. Note the high number of single labelled IdU^+ cells (red) after 0 h chase. These cells are activated during regeneration and entered S-phase during the second pulse (compare with 0h chase during homeostasis, Figure 2b). Note the gradually increasing amount of $CldU^+$ /IdU- cells (green) after 4h and 24h chase. Anterior is to the left. Scale bars: 50µm.

Supplementary Figure S1: Accumulation of mitotic cells in *M. lignano* after incubation in colchicine.
(a) Graphs representing the number of mitotic cells after incubation in three different concentrations of colchicine: low (0.001%, left panel), median (0.005%, middle panel), and high (0.010%, right panel). X-axis represents the incubation time in colchicine. Y-axis represents the mean number of mitotic cells (±SEM, n=4). For animals incubated in the median concentration, a significant higher number of mitotic cells (one-way ANOVA, p=0.01) was observed after 3h of colcichine-treatment, compared to the lowest concentration. The highest concentration was observed to cause a toxic effect for incubations longer than 24 hours, and no successful labelling could be performed. For animals treated with the middle and low concentration, such a toxic effect was not observed for incubations up to 48h. In conclusion, the use of a 0.005% solution of colchicine demonstrated a good balance between having a fast and efficient blocking of cells in M-phase on one hand, and experiencing no dramatic toxic effects for exposures up to 48h. This concentration was selected for further experiments. (b) Immunohistochemical labelling of mitotic cells using anti-phos-H3, after incubation in 0.005% colchicine.

Supplementary Figure S2: Tables representing the absolute numbers of the quantification data of the CldU/IdU double labelling during homeostasis and regeneration.
In the 1st and 2nd column the chase time duration and the number of replicates are given, respectively. The 3rd column represents the absolute numbers of double labelled cells ($CldU^+/IdU^+$). The 4th column demonstrates the total number of CldU-labelled cells ($CldU^+$), both single and double labelled. (a.) Homeostasis. Arrows and asterisks indicate significant (p=0.04, dotted arrow) and highly significant differences (p<0.01, arrows) in the number of $CldU^+$ cells. A significant increase of $CldU^+$ cells might be an indication of cell division of labelled cells, and thus inefficient blocking of cells in metaphase after prolonged incubations in colchicine (12 h). (b.) Regeneration. Significant differences in the number of $CldU^+$ cells are indicated (arrows and asterisks).

9. References

Agata K, Umesono Y. Brain regeneration from pluripotent stem cells in planarian. Philos Trans R Soc B-Biol Sci 2008;363(1500):2071-2078.

Alexiades MR, Cepko C. Quantitative analysis of proliferation and cell cycle length during development of the rat retina. Dev Dyn 1996;205(3):293-307.

Baguñà J. Planarian neoblasts. Nature 1981;290(5801):14-15.

Bolte S, Cordelieres FP. A guided tour into subcellular colocalization analysis in light microscopy. J Microsc 2006;224(Pt 3):213-232.

Borisy GG, Taylor EW. The mechanism of action of colchicine. Binding of colchincine-3H to cellular protein. J Cell Biol 1967;34(2):525-533.

Burns KA, Kuan CY. Low doses of bromo- and iododeoxyuridine produce near-saturation labeling of adult proliferative populations in the dentate gyrus. Eur J Neurosci 2005;21(3):803-807.

David CN, Campbell RD. Cell cycle kinetics and development of *Hydra attenuata* .1. Epithelial cells. J Cell Sci 1972;11(2):557-568.

De Vos WH, Van NL, Dieriks B, Joss GH, van OP. High content image cytometry in the context of subnuclear organization. Cytom Part A 2010;77(1):64-75.

Egger B, Ishida S. Chromosome fission or duplication in *Macrostomum lignano* (Macrostomorpha, Plathelminthes) - remarks on chromosome numbers in 'archoophoran turbellarians'. J Zool Syst Evol Res 2005;43(2):127-132.

Hayes NL, Nowakowski RS. Dynamics of cell proliferation in the adult dentate gyrus of two inbred strains of mice. Dev Brain Res 2002;134(1-2):77-85.

Kang H, Sánchez Alvarado A. Flow cytometry methods for the study of cell cycle parameters of planarian stem cells. Dev Dyn 2009;238(5):1111-1117.

Ladurner P, Egger B, De Mulder K, Pfister D, Kuales G, Salvenmoser W et al. The stem cell system of the basal flatworm *Macrostomum lignano*.In: Bosch ThCG, editors. Stem cells: from Hydra to man. Berlin - Heidelberg - New York: Springer;2008. p. 75-94.

Manders EMM, Stap J, Brakenhoff GJ, Vandriel R, Aten JA. Dynamics of three-dimensional replication patterns during the S-phase, analysed by double labelling of DNA and confocal microscopy. J Cell Sci 1992;103 (Pt 3)857-862.

Miller MA, Mazewski CM, Yousuf N, Sheikh Y, White LM, Yanik GA et al. Simultaneous immunohistochemical detection of IUdR and BrdU infused intravenously to cancer patients. J Histochem Cytochem 1991;39(4):407-412.

Morrison SJ, Shah NM, Anderson DJ. Regulatory mechanisms in stem cell biology. Cell 1997;88(3):287-298.

Morrison SJ, Spradling AC. Stem cells and niches: Mechanisms that promote stem cell maintenance throughout life. Cell 2008;132(4):598-611.

Nagl W. Selective-Inhibition of Cell Cycle Stages in Allium Root Meristem by Colchicine and Growth-Regulators. Am J Bot 1972;59(4):346-

Newmark PA, Sánchez Alvarado A. Bromodeoxyuridine specifically labels the regenerative stem cells of planarians. Dev Biol 2000;220(2):142-153.

Newmark PA, Sánchez Alvarado A. Not your father's planarian: A classic model enters the era of functional genomics. Nat Rev Genet 2002;3(3):210-219.

Nimeth KT, Egger B, Rieger R, Salvenmoser W, Peter R, Gschwentner R. Regeneration in *Macrostomum lignano* (Platyhelminthes): cellular dynamics in the neoblast stem cell system. Cell Tissue Res 2007;327(3):637-646.

Nimeth KT, Mahlknecht M, Mezzanato A, Peter R, Rieger R, Ladurner P. Stem cell dynamics during growth, feeding, and starvation in the basal flatworm *Macrostomum* sp. (Platyhelminthes). Dev Dyn 2004;230(1):91-99.

Orford KW, Scadden DT. Deconstructing stem cell self-renewal: genetic insights into cell-cycle regulation. Nat Rev Genet 2008;9(2):115-128.

Rachel RA, Dolen G, Hayes NL, Lu A, Erskine L, Nowakowski RS et al. Spatiotemporal features of early neuronogenesis differ in wild-type and albino mouse retina. J Neurosci 2002;22(11):4249-4263.

Rando TA. Stem cells, ageing and the quest for immortality. Nature 2006;441(7097):1080-1086.

Saló E, Baguñà J. Regeneration and pattern-formation in planarians .1. the pattern of mitosis in anterior and posterior regeneration in *Dugesia (G) tigrina*, and a new proposal for blastema formation. J Embryol Exp Morphol 1984;83(OCT):63-80.

Saló E, Baguñà J. Regeneration in Planarians and other worms: New findings, new tools, and new perspectives. J Exp Zool 2002;292(6):528-539.

Sánchez Alvarado A. Regeneration and the need for simpler model organisms. Philos Trans R Soc Lon Ser B-Biol Sci 2004;359(1445):759-763.

Sánchez Alvarado A. Stem cells and the planarian *Schmidtea mediterranea*. C R Biol 2007;330(6-7):498-503.

Schärer L, Knoflach D, Vizoso DB, Rieger G, Peintner U. Thraustochytrids as novel parasitic protists of marine free-living flatworms: *Thraustochytrium caudivorum* sp nov parasitizes *Macrostomum lignano*. Mar Biol 2007;152(5):1095-1104.

Schultz E, McCormick K. Skeletal muscle satellite cells. Ergeb Physiol 1994;123(-1):213-257.

Sokal RR, Rohlf FJ. Biometry the principles and practice of statistics in biological research. New York: W.H. Freeman and company;1995

Tanaka EM. Cell differentiation and cell fate during urodele tail and limb regeneration. Curr Opin Genet Dev 2003;13(5):497-501.

Taylor EW. The mechanism of colchicine inhibition of mitosis. I. Kinetics of inhibition and the binding of H3-colchicine. J Cell Biol 1965;25SUPPL-60.

Tsai RYL, Kittappa R, McKay RDG. Plasticity, niches, and the use of stem cells. Dev Cell 2002;2707-712.

Verdoodt F, Bert W, Couvreur M, De Mulder K, Willems M. Proliferative response of the stem cell system during regeneration of the rostrum in *Macrostomum lignano* (Platyhelminthes). Cell Tissue Res 2012a;347(2):397-406.

Verdoodt F, Willems M, Mouton S, De Mulder K, Bert W, Houthoofd W et al. Stem cells propagate their DNA by random segregation in the flatworm *Macrostomum lignano*. Plos One 2012b;7(1):e30227-

Villemont E, Dubois F, Sangwan RS, Vasseur G, Bourgeois Y, SangwanNorreel BS. Role of the host cell cycle in the Agrobacterium-mediated genetic transformation of Petunia: Evidence of an S-phase control mechanism for T-DNA transfer. Planta 1997;201(2):160-172.

Wenemoser D, Reddien PW. Planarian regeneration involves distinct stem cell responses to wounds and tissue absence. Dev Biol 2010;344(2):979-991.

West G, Inzé D, Beemster GTS. Cell Cycle Modulation in the Response of the Primary Root of Arabidopsis to Salt Stress. Plant Physiol 2004;135(2):1050-1058.

Willems M, Egger B, Wolff C, Mouton S, Houthoofd W, Fonderie P et al. Embryonic origins of hull cells in the flatworm *Macrostomum lignano* through cell lineage analysis: developmental and phylogenetic implications. Dev Genes Evol 2009;219(8):409-417.

Wimber DE, Quastler H. A ^{14}C- and ^{3}H-thymidine double labeling technique in the study of cell proliferation in *Tradescantia* root tips. Exp Cell Res 1963;30(1):8-22.

Yanik G, Yousuf N, Miller MA, Swerdlow SH, Lampkin B, Raza A. In vivo determination of cell cycle kinetics of non-Hodgkin's lymphomas using iododeoxyuridine and bromodeoxyuridine. J Histochem Cytochem 1992;40(5):723-728.

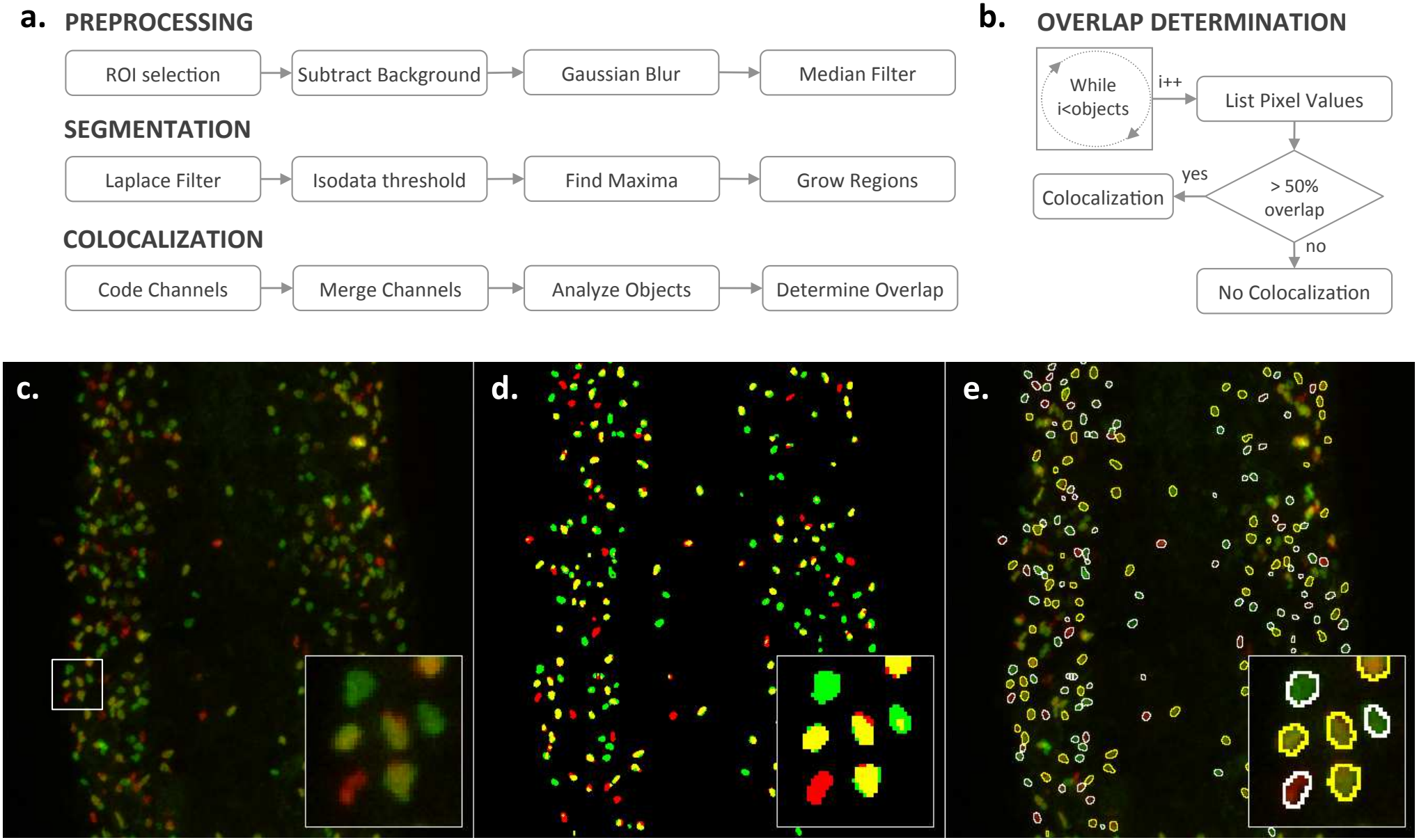
a.
PREPROCESSING
ROI selection
Subtract Background
Gaussian Blur
Median Filter
SEGMENTATION
Laplace Filter
Isodata threshold
Find Maxima
Grow Regions
COLOCALIZATION
Code Channels
Merge Channels
Analyze Objects
Determine Overlap
b.
OVERLAP DETERMINATION
While i<objects
i++
List Pixel Values
> 50% overlap
yes
Colocalization
no
No Colocalization
c.
d.
e.

Metric	CldU only (n=8)	IdU only (n=6)	IdU + CldU (n=8)
Pearson [-1,1]	0.10±0.03	0.25±0.08	0.79±0.12
Manders A [0,1]	0.07±0.03	0.14±0.12	0.52±0.08
Manders B [0,1]	0.03±0.03	0.08±0.04	0.35±0.14
Object-based [0,100] raw results	1.52±1.85	0.41±0.99	88.36±10.58
Object-based corrected [0,100] manually	0.0±0.00	0.00±0.00	91.91±8.17

Table 4.1: Comparison of the results from different colocalization metrics after intensity- or object based colocalization analysis on control image data sets.

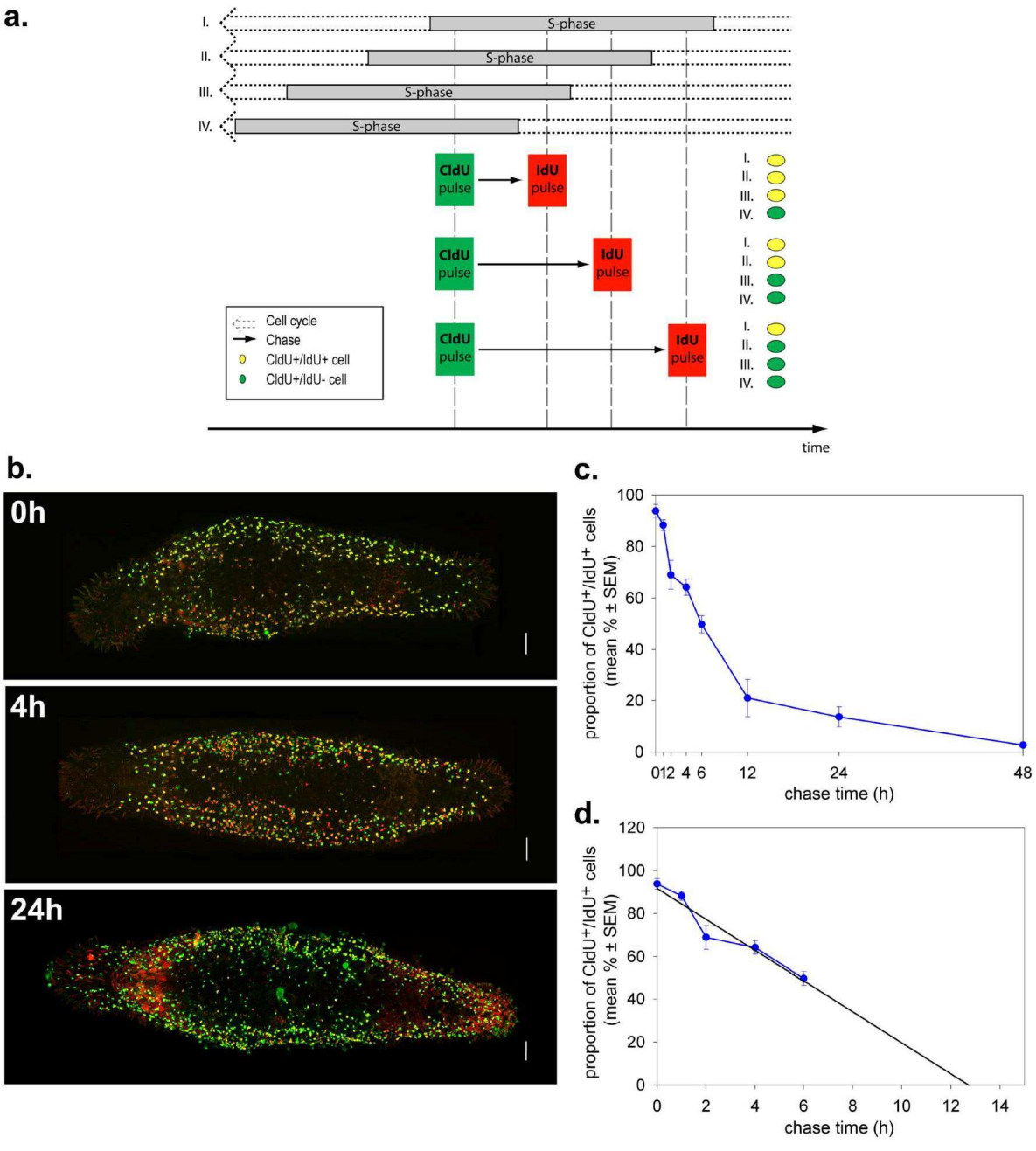
a.
I.
II.
III.
IV.
S-phase
CldU pulse
IdU pulse
Cell cycle
Chase
CldU+/IdU+ cell
CldU+/IdU- cell
time
b.
0h
4h
24h
c.
proportion of CldU+/IdU+ cells (mean % ± SEM)
chase time (h)
d.
proportion of CldU+/IdU+ cells (mean % ± SEM)
chase time (h)

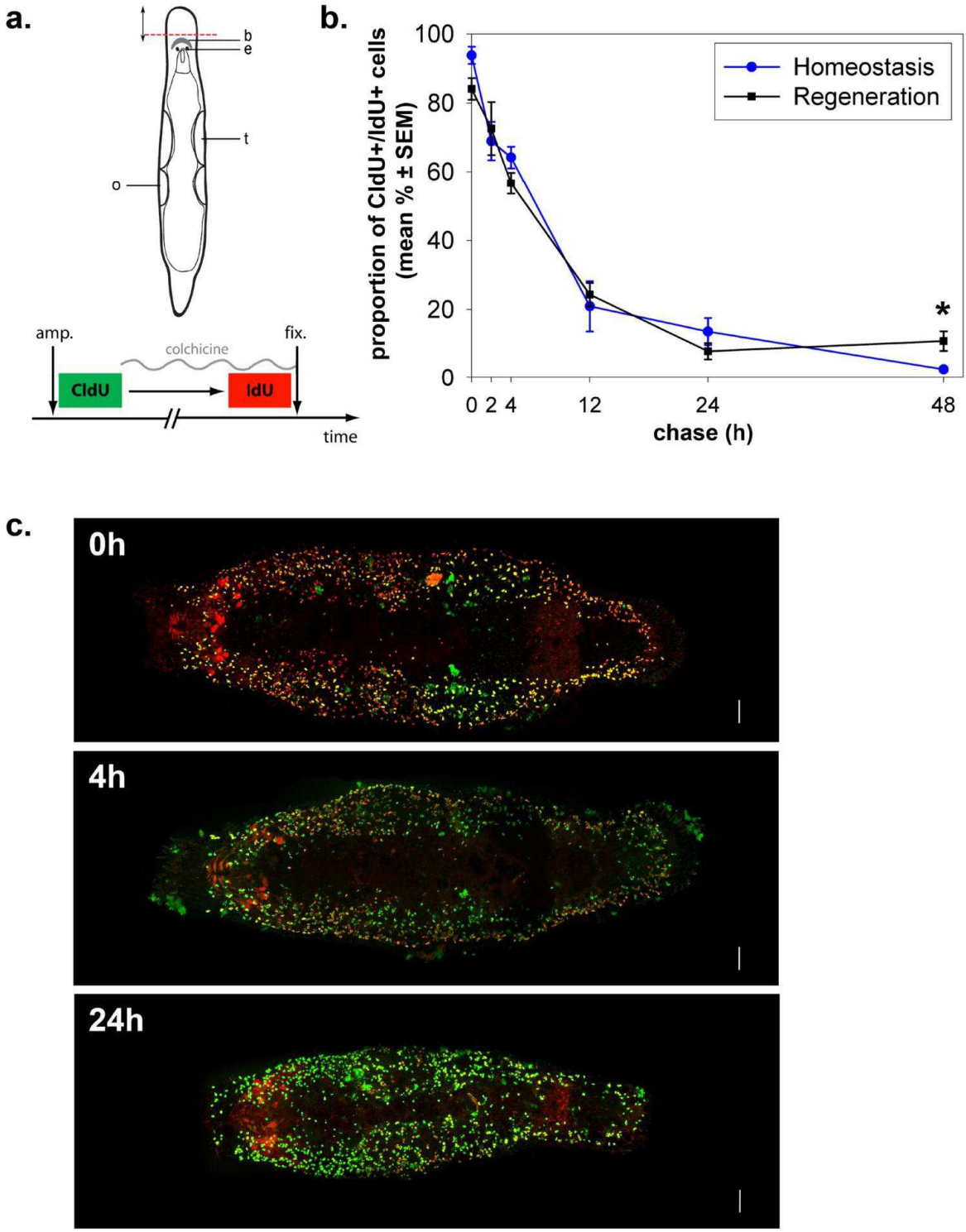
a.
b
e
t
o
amp.
fix.
colchicine
CldU
IdU
time
b.
proportion of CldU+/IdU+ cells
(mean % ± SEM)
100
80
60
40
20
0
Homeostasis
Regeneration
*
0 2 4
12
24
48
chase (h)
c.
0h
4h
24h